1   September 17, 2020 KB

2   **Fixation and effective size in a haploid-diploid population with asexual reproduction**

3

4   ***Kazuhiro Bessho, **Sarah P. Otto**

5   ** Saitama Medical University, 38 Morohongo Moroyama-machi, Iruma-gun, Saitama 350-0495,*

6   *Japan*

7   ***Department of Zoology, The University of British Columbia, Vancouver, BC, V6T 1Z4,*

8   *Canada*

9   * besshokazuhiro.reserch@gmail.com; (+81) 049-276-2030

10   ** otto@zoology.ubc.ca; (+1) 604-822-2778

11

12   (first version in bioRxiv, 17, September, 2020)

13

16

17

18 **Abstract**

19   The majority of population genetic theory assumes fully haploid or diploid organisms

20 with obligate sexuality, despite complex life cycles with alternating generations being commonly

21 observed. To reveal how natural selection and genetic drift shape the evolution of haploid-diploid

22 populations, we analyze a stochastic genetic model for populations that consist of a mixture of

23 haploid and diploid individuals, allowing for asexual reproduction and niche separation between

24 haploid and diploid stages. Applying a diffusion approximation, we derive the fixation

25 probability and describe its dependence on the reproductive values of haploid and diploid stages,

26 which depend strongly on the extent of asexual reproduction in each phase and on the ecological

27 differences between them.

28

1. Introduction

Sexual reproduction in eukaryotes generally consists of an alternation of generations, where meiosis halves the number of chromosomes to produce haploids and syngamy brings together haploid gametes to produce diploids. The extent of development in each ploidy phase varies substantially (Bell 1982; 1994). In diplontic organisms, at one extreme, development and growth occur only in the diploid phase, as is observed in most animals. Haplontic organisms, at the other extreme, undergo mitotic growth only in the haploid stage, as is seen in some green algae. In between these extremes, many terrestrial plants, macroalgae, and fungi exhibit both haploid and diploid growth (haploid-diploid life cycles). These stages are typically free living in macroalgae, with either macroscopically similar (isomorphic) or distinct (heteromorphic) forms in the haploid and diploid stage (Raper and Flexer 1970; Wilson 1981; Mable and Otto 1998; Coelho 2007).

To explain variation in life cycles, several theoretical models have analyzed the deterministic dynamics of a modifier allele that alters the time spent in haploid and diploid phases (e.g., Perrot et al. 1991; Otto and Goldstein 1992; Goldstein 1992; Otto 1994; Orr and Otto 1994; Jenkins and Kirkpatrick 1995; Otto and Marks 1996; Scott and Rescan 2017). However, there are some gaps between these models and the complexities seen in many haploid-diploid species. For example, these models often treat haploid and diploid individuals as ecologically equivalent, despite the frequent observation of niche differences and seasonal shifts in prevalence (e.g., Drew 1949; Slocum 1980; Dethier 1981). Most of these models also assume obligate sexuality (but see Otto and Marks 1996), despite asexuality being frequently observed among haploid-diploid species ("asexual looping"). Furthermore, while several models have explored how haploid-diploid life cycles might evolve, the impact of haploid-diploid life cycles

52   on evolutionary processes remains underexplored (see, e.g., Bessho and Otto 2017 on the impact

53   on fixation probabilities and Immler et al. 2012 on the maintenance of variation).

54   Here we contribute to evolutionary theory for haploid-diploid populations by

55   calculating the fixation probability of mutations using a stochastic genetic model. This builds

56   upon our previous work (Bessho and Otto 2017) by accounting for asexual looping and niche

57   differences between ploidy phases, both of which are common in macroalgae (Bell 1982; de

58   Wreede and Klinger 1988; Hawkes 1990). Haploid and diploid phases often differ

59   physiologically, and even isomorphic haploids and diploids may differ ecologically (Hannach

60   and Santelices 1985; Destombe et al. 1993; Dyck and de Wreede 2006; Thornber et al., 2006;

61   Vieira et al. 2018). We therefore explore different forms of density dependence, acting either

62   globally on the total population size (as in Bessho and Otto 2017) or locally on the population

63   size of haploids and diploids separately (Figure 1). We show that the fate of a mutation depends

64   strongly on the reproductive values of haploids and diploids, which in turn depend on the extent

65   of asexual reproduction and ecological differences between the phases.

66

67   **2. Model**

68   In Bessho and Otto (2017), we calculated the fixation probabilities by tracking the

69   dynamics of a resident allele (R) and a mutant allele (M) in haploid and diploid individuals, using

70   both a Wright-Fisher and a Moran model. In that model, reproduction was obligately sexual,

71   individuals were ecologically equivalent, and the total population size was held constant (global

72   density dependence). Below, we calculate the fixation probability by first considering asexual

73   reproduction in each phase, assuming that haploids and diploids are ecologically equivalent

74   (global population regulation), and then determine how these results are affected by niche

75   differences (local population regulation that is ploidy specific).

76

2.1. Haploid-diploid Wright-Fisher model with global regulation and asexual looping

78   Let $X_{(GT)}(t)$ be a random variable that represents the number of individuals with

79 "genotype" (GT) at time t with resident (R) and mutant alleles (M), and let $x_{(GT)}(t)$ represent a

80 particular outcome of this random variable. In the global regulation model, we assume a constant

81 population, $x_R + x_M + x_{RR} + x_{RM} + x_{MM} = N_{tot}$, that is strictly regulated regardless of the

82 ploidy of the individuals.

83   The reproductive output and the degree of asexuality are characterized by $w_{(GT)}$ and

84 a_H for haploids [(GT) = R or M] and $w_{(GT)}$ and a_D for diploids [(GT) = RR, RM, and MM].

85 Specifically, diploid individuals produce $(1 - a_D)w_{(GT)}$ haploid spores (sexual reproduction)

86 and $a_D w_{(GT)}$ diploid offspring (asexual loop). Similarly, haploids produce $(1 - a_H)w_{(GT)}/2$

87 female gametes (sexual reproduction) and $a_H w_{(GT)}$ haploid offspring (asexual loop), where we

88 assume that the species is monoecious and invests equal resources in male and female gametes.

89 During syngamy, we assume that male gametes are not limiting, that mating is random, and that

90 female gametes are successfully fertilized with male gametes, at a rate $f_{(GT)}$ [(GT) = R or M],

91 becoming diploid zygotes. For clarity, we describe the model with non-overlapping generations,

92 although we note that overlapping generations can be considered by including surviving adults in

93 the counts of asexual offspring ($a_D w_{(GT)}$ and $a_H w_{(GT)}$).

94   We define the selection coefficient ($s_{(GT)}$) and the degree of dominance (h) acting upon

95 the mutant allele such that: $f_M = f_R(1 - s_M^f)$, $w_M = w_R(1 - s_M^w)$, $w_{RM} = w_{RR}(1 - s_{RM}^w)$,

96 $w_{MM} = w_{RR}(1 - s_{MM}^w)$, and $h = s_{RM}^w/s_{MM}^w$. To perform the diffusion approximation, we assume

97 that selection is weak, $s_M^f = \epsilon \tilde{s}_M^f$ and $s_{(GT)}^w = \epsilon \tilde{s}_{(GT)}^w$, where ϵ is a small parameter.

98

2.2. Haploid-diploid Wright-Fisher model with local regulation and asexual looping

5

100   We then consider the case where density dependence regulates haploid and diploid

101   populations separately, which may occur if they have different resource needs or utilize different

102   habitats or microhabitats (for short-hand, we refer to this case as "local regulation"). More

103   specifically, we assume that the population size of haploids and diploids is separately regulated

104   and remains constant N_H and N_D ($x_R + x_M = N_H$ and $x_{RR} + x_{RM} + x_{MM} = N_D$), respectively.

105   We set $N_H + N_D = N_{tot}$, $\hat{\rho}_H^L = N_H/N_{tot}$, and $\hat{\rho}_D^L = N_D/N_{tot}$, which will then allow us to

106   compare the results of local and global regulation. Holding population sizes constant is assumed

107   strictly for mathematical convenience but may be reasonable for populations whose sizes are

108   strongly regulated by the availability of appropriate habitat.

109

110   **3. Fixation probability in a haploid-diploid population**

111   3.1. Fixation probability in the global regulation model

112   The fixation probability in a haploid-diploid population can be derived using a diffusion

113   approximation (Bessho and Otto 2017), but doing so requires that we approximate the dynamics

114   to reduce the dimensionality from four variables ($x_R, x_M, x_{RR}, x_{RM}, x_{MM}$, which sum to N_{tot}) down

115   to one. We do so by using a separation of time scales, deriving the first and second moments of the

116   mutant allele frequency. Specifically, we transform the number of individuals of each genotype,

117     $x_{(GT)}$, into new variables that allow us to separate the slower evolutionary dynamics and the faster

118   ecological dynamics (Appendix A):

$$p_{ave} = c_H\, p_H + c_D\, p_D, \tag{1a}$$

$$\delta_p = p_D - p_H, \tag{1b}$$

$$\eta_{HW} = 1 - \frac{1}{2p_D(1-p_D)}\frac{x_{RM}}{x_{RR} + x_{RM} + x_{MM}}, \tag{1c}$$

6

$$\rho_H = \frac{x_R + x_M}{N_{tot}},$$ (1d)

119 where p_{ave} indicates the average allele frequency of haploids and diploids weighted by the class

120 reproductive values (c_H and c_D, where $c_H + c_D = 1$, see next paragraph), δ_p indicates the

121 difference in allele frequencies between haploids and diploids, η_{HW} indicates the departure from

122 the Hardy-Weinberg equilibrium in diploids, and ρ_H indicates the frequency of haploids in the

123 population. Within these equations, the frequencies of mutant alleles in haploids and diploids are

124 $p_H = x_M/(x_R + x_M)$ and $p_D = \left(\frac{x_{RM}}{2} + x_{MM}\right)/(x_{RR} + x_{RM} + x_{MM})$. As similar variables are

125 used in the model with local population regulation, we use superscripts to indicate the form of

126 population regulation ("*Model*" is *G* for global or *L* for local regulation).

127   The class reproductive values of haploids and diploids are defined as follows. In linear

128 models, "reproductive value" is a measure of the expected fraction of the population in the long-

129 term future that descends from an individual of a particular type (e.g., age or stage class). Class

130 reproductive values, as defined by Taylor (1990) and Rousset (2004, p.153), scale these individual

131 reproductive values up to the whole population of each class (i.e., the product of the individual

132 reproductive values times the class size). In the models considered here, the dynamics are non-

133 linear because of competition for resources (N_{tot}). Nevertheless, we can approximate reproductive

134 values by assuming that the population is near equilibrium with only resident alleles and by holding

135 the strength of competition constant (see Supplementary *Mathematica* file for all calculations).

136 Doing so, we find that the class reproductive values of haploids and diploids, expressed as

137 proportions that sum to one, are:

$$c_H^G = \frac{(1 - a_H)\frac{f_R}{2}w_R(\hat\rho_H^G)^2}{(1 - a_H)\frac{f_R}{2}w_R(\hat\rho_H^G)^2 + (1 - a_D)w_{RR}(\hat\rho_D^G)^2},$$ (2a)

7

$$c_D^G = \frac{(1-a_D)w_{RR}(\hat{\rho}_D^G)^2}{(1-a_H)\frac{f_R}{2}w_R(\hat{\rho}_H^G)^2 + (1-a_D)w_{RR}(\hat{\rho}_D^G)^2}. \tag{2b}$$

138   where $\hat{\rho}_H^G = 1 - \hat{\rho}_D^G$ is the equilibrium frequency of haploids in the global model (Eq. A.4). As a

139   special case of interest, when populations are purely sexual ($a_H = a_D = 0$), we can plug the

140   equilibrium for $\hat{\rho}_H^G$ from Eq. (A.4) into (2) and show that $c_H^G = c_D^G = 1/2$.

141   As discussed in Appendix A (see also Bessho and Otto 2017), equations (2) provide the

142   only weights that allow ecological and evolutionary time scales to be separated when calculating

143   the average allele frequency in equation (1a), which is why we take that to be the evolutionarily

144   relevant average. Although one might initially think that diploids should count twice as much

145   because they contain two allele copies and that the evolutionarily relevant average allele frequency

146   would depend on the population sizes of haploids and diploids, a strict alternation of generations

147   ($a_H = a_D = 0$) ensures that haploids and diploids contribute equally to long-term future

148   generations, so that their reproductive values are equal and the evolutionarily relevant average

149   allele frequency is $p_{ave} = (1/2)p_H + (1/2)p_D$ (Bessho and Otto 2017).

150   As with our previous model, we can track the slow evolutionary dynamics for the

151   expected change in average allele frequency p_{ave} under weak selection, once the fast ecological

152   dynamics have stabilized, as which point we can show that there are similar allele frequencies in

153   haploids and diploids ($\delta_p \approx 0$), diploids are approximately at Hardy-Weinberg equilibrium

154   ($\eta_{HW} \approx 0$), and the ratio of haploids is similar among mutant and resident genotypes ($\rho_H \approx \hat{\rho}_H^G$)

155   (Appendix A, File S1). Furthermore, to leading order, the second moment of change in allele

156   frequency is equal to the neutral case and can be derived in the diffusion limit ($N_{tot} \to \infty$).

157   Given a single variable, p_{ave}, changing slowly over evolutionary time, we can then use

158   standard diffusion methods to calculate the fixation probability of a mutation in a haploid-diploid

159   population, $u(p_0^{Model})$, where "*Model*" is G for global and L for local (considered in the next

8

160   section). The diffusion is a function of the first and second moments of change in the mutant allele

161   frequency, $m^{Model}(p_{ave})$ and $v^{Model}(p_{ave})$, both measured in time units of N_{tot} generations:

$$u\left(p_0^{Model}\right) = \frac{\int_0^{p_0^{Model}} \exp[-2Q^{Model}(p')]\,dp'}{\int_0^1 \exp[-2Q^{Model}(p')]\,dp'}, \tag{3a}$$

$$m^{Model}(p_{ave}) = \frac{N_{tot}\,p_{ave}(1-p_{ave})}{2}\left[2s_{ave}^{Model} + 2c_D^{Model}p_{ave}(1-2h)s_{MM}^w\right], \tag{3b}$$

$$v^{Model}(p_{ave}) = \frac{p_{ave}(1-p_{ave})\left[\left(c_D^{Model}\right)^2\widehat{\rho}_H^{Model} + \left(c_H^{Model}\right)^2\left(2\widehat{\rho}_D^{Model}\right)\right]}{\widehat{\rho}_H^{Model}\left(2\widehat{\rho}_D^{Model}\right)}. \tag{3c}$$

162   where p_0^{Model} is the initial allele frequency of mutants (we focus on the case with a single initial

163   mutant   allele, $p_0^{Model} = 1/\left[N_{tot}\left(\widehat{\rho}_H^{Model} + 2\widehat{\rho}_D^{Model}\right)\right]$)   and $Q^{Model}(p) =$

164    $\int\left(m^{Model}(p)/v^{Model}(p)\right)dp$. For the global regulation model, the average selection acting upon

165   rare mutant alleles across haploid and diploid stages, s_{ave}^G, can be calculated from the first moment

166   equation (Appendix 1) and equals:

$$s_{ave}^{Model} = c_H^{Model}s_M^w + c_D^{Model}s_{RM}^w + \phi^{Model}c_D^{Model}\frac{s_M^f}{2}, \tag{4a}$$

$$\phi^{Model} = \frac{(1-a_H)\widetilde{w}_R\widehat{\rho}_H^{Model}}{(1-a_H)\widetilde{w}_R\widehat{\rho}_H^{Model} + a_D w_{RR}\widehat{\rho}_D^{Model}}. \tag{4b}$$

167   where $\widetilde{w}_R = f_R w_R/2$ is the fitness of haploids considering the cost of sex. As we will see later,

168   this equation is valid for local regulation model. The term ϕ^{Model} indicates the fraction of the

169   diploids in the next generation that come from the union of gametes rather than diploid asexual

170   reproduction. With obligately sexual haploid-diploids ($a_H = a_D = 0$, where $c_H^{Model} = c_D^{Model} =$

171    $1/2$ and $\phi^{Model} = 1$), these results coincide with those of Bessho and Otto (2017).

172

173   3.2. Fixation probability in the local regulation model

174   We next derive the fixation probability in a haploid-diploid population when density

175   dependence regulates haploid and diploid populations separately (Figure 1b), by again applying a

9

176 transformation of variables and separation of time scales. For the local regulation model, the

177 appropriate weights for the average allele frequency are similar to the global regulation model,

178 where now the class reproductive values, expressed as proportions, are:

$$c_H^L = \frac{1 + \dfrac{a_H w_R \hat{\rho}_H^L}{(1-a_D)w_{RR}\hat{\rho}_D^L}}{2 + \dfrac{a_H w_R \hat{\rho}_H^L}{(1-a_D)w_{RR}\hat{\rho}_D^L} + \dfrac{2}{f_R}\dfrac{a_D w_{RR}\hat{\rho}_D^L}{(1-a_H)w_R \hat{\rho}_H^L}}, \tag{5a}$$

$$c_D^L = \frac{1 + \dfrac{2}{f_R}\dfrac{a_D w_{RR}\hat{\rho}_D^L}{(1-a_H)w_R \hat{\rho}_H^L}}{2 + \dfrac{a_H w_R \hat{\rho}_H^L}{(1-a_D)w_{RR}\hat{\rho}_D^L} + \dfrac{2}{f_R}\dfrac{a_D w_{RR}\hat{\rho}_D^L}{(1-a_H)w_R \hat{\rho}_H^L}}. \tag{5b}$$

179

180 After applying a separation of time scales and conducting a diffusion approximation, we conclude

181 that the solution for the fixation probability in a haploid-diploid population, Eqs. (3), remains valid

182 for the local regulation model (Supplementary *Mathematica* file), with the average selection

183 coefficient now being given by Eqs. (5).

184

185 3.3. Effective genetic parameters

186 Using the first and second moments of change in allele frequency, we derive effective

187 genetic parameters to compare our results to the dynamics found in the classical model for fully

188 haploid or fully diploid organisms (Bessho and Otto 2017). More specifically, we define the

189 effective selection coefficient (s_e), dominance coefficient (h_e), and effective population size (N_e)

190 that would result in the same expected change in allele frequency and variance as in the classical

191 diploid model of selection.

192 For selection, the diploid model is: $\Delta p_{ave} = s_e p_{ave}(1 - p_{ave})[h_e + (1 - 2h_e)p_{ave}]$

193 (Crow and Kimura 1970; Bessho and Otto 2017). Because this equation depends on the allele

194 frequency in the same way as Eq. (3b), we can find the effective and dominance selection

10

195   coefficient   from $\Delta p_{ave}/[p_{ave}(1 - p_{ave})] = s_e h_e$ when $p_{ave} = 0$ and

196     $\Delta p_{ave}/[p_{ave}(1 - p_{ave})] = s_e(1 - h_e)$ when $p_{ave} = 1$, yielding:

$$s_e^{Model} = 2s_{ave}^{Model} + 2\hat{c}_D^{Model}\frac{(1 - 2h)s_{MM}^w}{2}. \tag{6a}$$

$$h_e^{Model} = \frac{2s_{ave}^{Model}}{4s_{ave}^{Model} + 2\hat{c}_D^{Model}(1 - 2h)s_{MM}^w}. \tag{6b}$$

197   When the mutation is additive ($h = 1/2$), these effective parameters are $s_e^{Model} = 2s_{ave}^{Model}$ and

198     $h_e^{Model} = 1/2$.

199   We next derive the variance effective population size by equating the one generation

200   change in variance (Eq. 3c divided by the time scale, N_{tot}) to the variance in allele frequency

201   expected in the classical Wright-Fisher model, $p_{ave}(1 - p_{ave})/2N_e$ with N_e diploid individuals,

202   obtaining:

$$N_e^{Model} = \frac{p_{ave}(1 - p_{ave})}{2(v^{Model}/N_{tot})} = \frac{N_{tot}\,\hat{\rho}_H^{Model}\hat{\rho}_D^{Model}}{(c_D^{Model})^2\hat{\rho}_H^{Model} + 2(c_H^{Model})^2\hat{\rho}_D^{Model}}. \tag{7}$$

203   Plugging these effective parameters into the formula from the fixation probability in the

204   classical diploid Wright-Fisher model (Kimura 1957; 1962; Crow and Kimura 1970, p. 427), the

205   fixation probability in a haploid-diploid population given by Eq. 3a can be expressed as:

$$u(p_0^{Model}) = \frac{\int_0^{p_0^{Model}} \exp[-2N_e^{Model}s_e^{Model}\{(2h_e^{Model} - 1)p'(1 - p') + p'\}]\,dp'}{\int_0^1 \exp[-2N_e^{Model}s_e^{Model}\{(2h_e^{Model} - 1)p'(1 - p') + p'\}]\,dp'}. \tag{8}$$

206   Assuming an initially rare and additive mutation ($h = 1/2$) with weak positive selection in a large

207   population ($s_e^{Model}N_e^{Model}p_0^{Model} \approx 0$ and $s_e^{Model}N_e^{Model} \gg 1$), we obtain the classic

208   approximation, $u(p_0^{Model}) \approx 2s_e^{Model}N_e^{Model}p_0^{Model}$, which upon substituting from Eq. 7 yields:

$$u(p_0^{Model}) \approx \frac{2\hat{\rho}_H^{Model}\hat{\rho}_D^{Model}}{(\hat{\rho}_H^{Model} + 2\hat{\rho}_D^{Model})\left[(c_D^{Model})^2\hat{\rho}_H^{Model} + 2(c_H^{Model})^2\hat{\rho}_D^{Model}\right]}2s_{ave}^{Model}. \tag{9a}$$

209   For example, because haploids and diploids have the same reproductive values in the obligately

210   sexual case ($\hat{c}_H^{Model} = \hat{c}_D^{Model} = 1/2$), we obtain:

$$u(p_0^{Model}) \approx \frac{8\hat{\rho}_H^{Model}\hat{\rho}_D^{Model}}{(\hat{\rho}_H^{Model} + 2\hat{\rho}_D^{Model})^2}\,2s_{ave}^{Model} \tag{9b}$$

11

211 (Eq. 13a in Bessho and Otto 2017), or simply $u\left(p_0^{Model}\right) \approx 2s_{ave}^{Model}$ if haploid and diploid

212 population sizes are equal in terms of number of chromosomes ($\hat{\rho}_H^{Model} = 2/3$).

213   In the next three sections, we explore the implications of these results for the evolution

214 of haploid-diploid populations.

215

216 3.4. Effective selection in a haploid-diploid population

217   The strength of selection averaged across haploids and diploids, s_{ave}^{Model}, plays a key

218 role in the evolution of haploid-diploid populations. When a mutation is rare, both the rate of

219 change in allele frequency (Eq. 3b) and the approximate fixation probability (Eq. 10a) are

220 proportional to s_{ave}^{Model}. We thus begin by exploring how s_{ave}^{Model} varies as we alter the amount of

221 asexual reproduction in haploid and diploid phases. We focus on the case where the mutation does

222 not affect fertilization success ($s_M^f = 0$), so that the average selection becomes:

$$s_{ave}^{Model} = c_H^{Model} s_M^W + c_D^{Model} s_{RM}^W, \tag{10}$$

223 in both global and local regulation models (Eqs. (4) and (6)).

224   The relative evolutionary importance of selection in the haploid and diploid phases is

225 thus determined by the class reproductive values, c_H^{Model} and c_D^{Model} (where $c_H^{Model} +$

226 $c_D^{Model} = 1$). Figures 2 (global regulation) and 3 (local regulation) illustrate the proportional

227 reproductive value of haploids, c_H^{Model}, as a function of the degree of asexual reproduction in

228 haploids (x-axis) and diploids (ranging from 0.05 in red to 0.95 in blue). With global regulation,

229 the frequency of haploidy within the population, $\hat{\rho}_H^G$ (given by Eq. A.4), varies with the

230 parameters (see inset graphs in Figure 2), rising with the frequency of haploid asexuality (x-axis

231 in inset) but declining with more asexuality in diploids (from red to blue). By contrast, with local

232 regulation, the frequency of haploidy is held fixed by the strict density dependent competition that

233 we have assumed ($\hat{\rho}_H^L = 0.8$ in Figure 3(a)(b) and 0.3 in 3(c)(d)).

234   In the left panels, haploids have a higher fertility ($w_R/w_{RR} = 5$), leading to a higher

235   haploid reproductive value, c_H^{Model}, especially with local regulation when haploids are also more

236   common ($\hat{\rho}_H^L = 0.8$ in Figure 3a). In the right panels, diploids have a higher fertility ($w_{RR}/w_R = $

237   5), leading to a lower haploid reproductive value, especially when haploids are rare ($\hat{\rho}_H^L = 0.3$ in

238   Figure 3d).

239   When haploids are primarily sexual ($a_H \approx 0$), increasing asexuality of the haploid stage

240   typically causes the reproductive value of haploids to rise, unless diploids are fitter and more

241   frequent (Figure 3d and blue curves in Figure 2b). At the other extreme, the reproductive value of

242   haploids typically plummets to zero as haploid reproduction becomes primarily asexual ($a_H \approx 1$)

243   while diploids remain sexual, particularly with local regulation (Figure 3), because haploids then

244   act as a genetic "sink" contributing little to the diploid sub-population. This downward trend when

245   haploids are predominantly asexual is also seen with global regulation if diploids are more fit

246   (Figure 2b), except when the diploid population does not sustain itself and goes extinct, which

247   occurs when $a_D < 0.2$ and $a_H = 1$. The net result can thus be non-monotonic (purple curves

248   with $0.2 < a_D < 0.4$ in Figure 2b and Figure 3(a)(b)(c)).

249

250   3.4. Effective population size in a haploid-diploid population

251   We next consider the effective size of haploid-diploid populations with varying degrees

252   of asexuality. Figure 4 plots the effective population size (Eq. 8) relative to the total population

253   size, N_e^{Model}/N_{tot}, as a function of the frequency of haploids, $\hat{\rho}_H^{Model}$ (x-axis), and the class

254   reproductive values (with c_H^{Model} ranging from 0.05 in blue to 0.95 in red). As noted by Bessho

255   and Otto (2017), the effective population size is highest – and drift weakest – at intermediate

256   frequencies of haploids and diploids, which ensures the least sampling error as organisms alternate

257   generations.

13

258   When haploids and diploids have equal reproductive values, as in the fully sexual case

259   ($c_H^{Model} = c_D^{Model} = 1/2$), the effective population size is maximized at $\hat{\rho}_H^{Model} \approx 0.586$. With

260   asexual reproduction, the peak shifts towards whichever ploidy level has the higher reproductive

261   value. For example, if haploids have a high reproductive value (red) then the effective population

262   size is maximized at a higher frequency of haploids, reducing the amount of genetic drift in that

263   phase. Although not illustrated, the peak shifts to $N_e^{Model} = \hat{\rho}_D^{Model} N_{tot}$ when future populations

264   descend only from diploids ($c_H^{Model} = 0$) and to $N_e^{Model} = (\hat{\rho}_H^{Model}/2)N_{tot}$ when future

265   populations descend only from haploids ($c_H^{Model} = 1$), effectively becoming diplontic or haplontic,

266   respectively (with the $1/2$ arising because haploids have half the number of chromosomes).

267   Of course, the reproductive values, as well as the frequency of haploids with global

268   population regulation ($\hat{\rho}_H^G$), depend in turn on the fitness parameters and the extent of asexuality,

269   as explored in the previous section. Figures 5 (global regulation) and 6 (local regulation) illustrate

270   the effective population size as a function of the frequency of haploid asexuality, a_H (x-axis), and

271   the frequency of diploid asexuality (a_D rising from red to blue), using the parameters in Figures 2

272   and 3, respectively. The trends are often non-monotonic, with N_e^{Model}/N_{tot} values varying

273   around $1/2$ when the parameter values are intermediate. The effective population size is often

274   higher when diploids rarely reproduce asexually (red) rather than when they frequently do (blue),

275   although there are exceptions (particularly when the fitness and frequency of diploids is high).

276

277   3.6. Fixation probability in a haploid-diploid population

278   We next compare the above results with numerical simulations estimating the fixation

279   probability of a newly arisen mutation in a haploid-diploid population. When simulating the global

280   regulation model, we assumed that the population has reached the demographic equilibrium,

281    $\hat{\rho}_H^G N_{tot}$ haploids and $\hat{\rho}_D^G N_{tot}$ diploids (see Appendix A). We then chose one resident allele R at

14

282   random and replaced it with a mutant allele M. After mutation, offspring were sampled from the

283   parental generation according to a multinomial distribution with expected frequencies given by

284    $x_{(GT)}$, repeating until the mutant allele fixed or was lost from the population. We estimated the

285   fixation probability as the fraction of 10,000 replicate simulations leading to fixation.

286   We here consider the additive case ($h = 1/2$ and $h_e = 1/2$), where the fixation

287   probability (Eq. 8) simplifies to:

$$u\left(p_0^{Model}\right) = \frac{\exp[-2p_0^{Model}N_e^{Model}s_e^{Model}] - 1}{\exp[-2N_e^{Model}s_e^{Model}] - 1} \tag{11}$$

288   and where $s_e^{Model} = 2\,s_{ave}^{Model}$ (Eq. 6). Figure 7 plots the fixation probability as a function of the

289   average selection pressure, s_{ave}^{Model}, when the reproductive values and chromosome numbers in

290   haploids and diploids are equal ($c_H^{Model} = c_D^{Model}$ and $\hat{\rho}_H^{Model} = 2/3$) and $s_{ave}^{Model} = [(1/2)s_M^w +$

291    $(1/2)s_{RM}^w]$. The diffusion Eq. (11) provides an excellent fit, as does the approximation Eq. (9b)

292   for selection coefficients that are positive and not too weak. In this case, the results are the same

293   with global and local population regulation (Fig. 7a and 7b, respectively) and are insensitive to

294   how much selection occurs in the haploid or diploid phases (s_M^{Model} and s_{RM}^{Model}, respectively), as

295   long as s_{ave}^{Model} is held constant (see additional simulations in Supplementary *Mathematica* file).

296   As expected, the extent of selection in the haploid versus diploid phase matters more when the

297   mutation is not additive ($h \neq 1/2$ and $h_e \neq 1/2$) (supplementary *Mathematica* file).

298   Next, we illustrate the approximate fixation probability, Eq. (9a), as a function of the

299   degree of asexuality (a_H and a_D) when the population size is globally (Fig. 8) or locally (Fig. 9)

300   regulated, assuming only selection in haploids or only in diploids. For example, with additive

301   mutations, the fixation probability can be approximated as $u \approx 4c_H^{Model}N_e^{Model}p_0^{Model}s_M^w$ when

302   selection occurs only in the haploid phase or $u \approx 4c_D^{Model}N_e^{Model}p_0^{Model}s_{RM}^w$ with selection only

303   in the diploid phase, indicating that the fate of mutations depends as much on the strength of

304   selection as on the reproductive value of the ploidy phase in which selection acts (as illustrated in

15

305   Fig. 2 and 3). Figures 8 (global) and 9 (local) illustrate how the fixation probability depends on the

306   various parameters in the model, particularly the amount of asexual reproduction in haploids (x-

307   axis) and diploids (a_D rising from red to blue). The trends can be understood by the combined

308   effects of the parameters on the reproductive value and the effective population size (e.g., Fig. 9(a)

309   is proportional to the product of Fig. 3(a) and Fig. 6(c)).

310

311   **4. Discussion**

312   Across the phylogenetic tree of life, organisms have diverse and complex reproductive

313   strategies (Bell 1982). Classical population genetic theory has, however, focused most on fully

314   haploid or diploid life cycles with obligate sexuality. In this article we develop a stochastic model

315   for the population genetics of haploid-diploid organisms considering demography, asexuality, and

316   habitat differentiation between haploid and diploid stages. Using a separation of time scales, we

317   derive a diffusion approximation for the change in allele frequency, allowing us to estimate the

318   fixation probability of new mutations, the effective strengths of selection and dominance, as well

319   as the effective population size of haploid-diploid populations.

320

321   5.1. Natural selection in a haploid-diploid population

322   Our results indicate that the strength of natural selection and the extent of genetic drift

323   depend strongly on the reproductive value of haploid versus diploid phases. In the simplest case,

324   when the effect of a mutation is weak, additive, positive, and absent in the gamete stage ($s_M^f = 0$),

325   the fixation probability is proportional to the effective strength of selection (Eq. 10), $s_e^{Model} =$

326    $2s_{ave}^{Model}$, which in turn is proportional to the amount of selection in and the reproductive value of

327   haploids and diploids (Eqs. 2, and 5).

328   These analytical results reveal some evolutionary principles for populations that undergo

16

329   an alternation of generations. One consequence is that the balance of opposing selection pressures

330   in haploids and diploids (Eqs. 4 and 6) depends not only on the selection coefficients, but also on

331   the relative reproductive values of haploids (c_H^{Model}) versus diploids (c_D^{Model}). Thus, the very

332   direction of evolution depends on the extent of asexuality in the two phases and the relative survival

333   and fertility of haploids versus diploids when there is "ploidally antagonistic selection" (Immler et

334   al. 2012).

335   The efficacy of selection to fine tune traits in haploids and diploids also depends on the

336   class reproductive values. For example, when the population is regulated by local density

337   dependence (i.e., the haploid and diploid phases are spatially or temporally distinct), higher

338   reproductive success in haploids increases the efficiency of haploid selection (compare Figure 3a

339   to 3b). However, when there is extremely rare sexuality in haploids (a_H near one), diploid

340   selection tends to be more effective because of increasing competition between offspring from

341   haploids. By contrast, the trends differ with global density dependence (e.g., species that are more

342   isomorphic with small ecological differences between stages). For example, the reproductive value

343   of haploids remains high even when they reproduce primarily asexually in the global regulation

344   model (see Figure 2 when a_H approaches one), because haploids then make up a larger proportion

345   of the total population size (see inset figures). Thus, whether selection is effective in the haploid

346   phase when that phase mainly reproduces asexually is quite sensitive to the nature of competition.

347   Our work can also be useful in the design of field studies and the interpretation of data

348   for species that alternate generations. To understand the efficiency of selection on haploid and

349   diploid phases, we not only need data about the fraction of haploids and diploids and their fertility

350   and mortality (e.g., Thornber and Gains 2004; Vieira et al., 2018a; Vieira et al. 2018b), but we also

351   need to know about the extent of asexuality in each phase and whether they compete for common

352   or different resources.

353

354 5.2. Genetic drift and effective size

355 The impact of random genetic drift on the genetic diversity of haploid-diploid population

356 depends on the effective population size (Eq. 7). As we had found previously in a haploid-diploid

357 model with obligate sexuality (Bessho and Otto 2017, pp. 431), the effective population size with

358 asexuality is generally smaller than the total number of individuals and again depends strongly on

359 the reproductive value of each phase (Figures 4-6). With obligate sexuality, the reproductive values

360 of haploids and diploids are equal, and the effective population size is maximized (drift minimized)

361 when haploids comprise 2/3 of the population, making the number of chromosomes equal between

362 haploids and diploids. Asexual reproduction, however, causes the reproductive value of haploids

363 and diploids to differ (Eqs. 2 and 5). Consequently, drift is lessened if the phase with the higher

364 reproductive value is more common (see shifts in peaks in Figure 4).

365

366 5.3. "Ploidally-structured" population

367 The key role that reproductive values play in this work is analogous to the role that patch

368 dynamics play in two-patch models of evolution. In a spatially structured population, subdivided

369 local populations are genetically connected by migration. A haploid-diploid system can be seen as

370 being ploidally structured, where gene flow describes the movement of alleles through sexual

371 reproduction, with meiosis causing flow to haploidy and syngamy flow to diploidy. We note that

372 our research reveals that all qualitative results are equally accurate for evolution in a two-patch

373 system (see Supplementary *Mathematica* File). For example, fixation probability strongly depends

374 on class reproductive values of each patch.

375 This analogy suggests an interesting idea: complex reproductive systems can be

376 considered and analyzed using the tools of metapopulation theory. For example, many eukaryotes

377   including terrestrial plants, insects, and fishes, often exhibit ploidy variation, including polyploid

378   members (Otto and Whitton 2000; Comai 2005). In such species, individuals characterized by

379   different numbers of chromosomes coexist, with complex reproductive relationships causing gene

380   flow between them (Ramsey and Schemske 1998). Similarly, social insects often exhibit complex

381   sex determination systems linked with ploidy levels (haplodiploidy).

382   Our research suggests that these ploidally-structured populations can be fruitfully treated

383   as metapopulations. Selection and drift in populations with diploids, triploids, and tetraploids can,

384   for example, be considered as a three-patch model. In this system, we conjecture that the average

385   strength of selection that is evolutionarily relevant would be the mean selection coefficient in each

386   ploidy class, weighted by its class reproductive value, with additional terms coming from

387   reproductive interactions (akin to the term of s_M^f in Eqs. 4).

388   Many evolutionary aspects of haploid-diploid populations remain to be investigated. One

389   avenue that we are exploring is how model parameters can be estimated from field data. For

390   example, the analogy between spatially and ploidally structured population suggests that genetic

391   differences between haploids and diploid can be used to estimate gene flow between them (i.e.,

392   rates of sex), akin to using Fst to inform estimates of migration (e.g., Slatkin 1987). Another fruitful

393   avenue for further work is to determine how fluctuations in population size affect the effective

394   population size of species that alternate generations. In classical population genetics theory, such

395   fluctuations can be captured by using the harmonic mean population in place of the total population

396   size (Karlin 1968). It is unclear, however, whether the same is true in haploid-diploid populations.

397   Can the harmonic total population size simply replace N_{tot} in the global model of population

398   regulation? Similarly, can the harmonic population sizes of haploids and diploids replace N_H and

399   N_D with local regulation? The answer is unclear because population size fluctuations perturb the

400   fast ecological dynamics away from the steady state (especially $\hat{\rho}_H^{Model}$), and the impact of these

19

401 perturbations on selection and drift is unknown. Further research is needed to clarify evolutionary

402 processes in the wide variety of species that alternate generations.

403

404 **Acknowledgements**

409

410 **Appendix A. Fixation probability in a haploid-diploid Wright-Fisher model using a**

411 **diffusion approximation**

412 A.1. Equilibrium with global regulation

413 We derive the fixation probability in a haploid-diploid population using a diffusion

414 approximation (e.g., Bessho and Otto 2017). We first derive the stable equilibrium in the global

415 regulation model, allowing for asexual reproduction in each phase. In the Wright-Fisher model,

416 all individuals reproduce and then the parents die (non-overlapping generations). Let $b_{(GT)}$

417 represent the number of reproductive cells of each type in the next generation:

$$b_R = (1-a_D)w_{RR}x_{RR} + (1-a_D)\frac{w_{RM}x_{RM}}{2} + a_H w_R x_R, \tag{A.1a}$$

$$b_M = (1-a_D)\frac{w_{RM}x_{RM}}{2} + (1-a_D)w_{MM}x_{MM} + a_H w_M x_M, \tag{A.1b}$$

$$b_{RR} = (1-a_H)\frac{f_R}{2}\frac{w_R^2 x_R^2}{w_R x_R + w_M x_M} + a_D w_{RR}x_{RR}, \tag{A.1c}$$

$$b_{RM} = (1-a_H)\frac{f_R + f_M}{2}\frac{w_R w_M x_R x_M}{w_R x_R + w_M x_M} + a_D w_{RM}x_{RM}, \tag{A.1d}$$

$$b_{MM} = (1-a_H)\frac{f_M}{2}\frac{w_M^2 x_M^2}{w_R x_R + w_M x_M} + a_D w_{MM}x_{MM}. \tag{A.1e}$$

20

418 The probability that a reproductive cell of genotype (GT) is sampled from the offspring produced

419 by the previous generation of adults is

$$q_{(GT)} = \frac{b_{(GT)}}{b_R + b_M + b_{RR} + b_{RM} + b_{MM}}. \qquad (A.2)$$

420 Therefore, the composition of offspring in the next generation is given by the multinomial

421 distribution, sampling N_{tot} individuals in proportion to Eq. (A2). Using Eq. (A1) and (A2), we

422 describe the conditional expectation of change in the number of individuals of genotype (GT),

423 $\Delta X_{(GT)}(t) = X_{(GT)}(t+1) - X_{(GT)}(t)$, as

$$E\big[\Delta X_{(GT)}(t) | \vec{X}(t) = \vec{x}\big] = N_{tot} q_{(GT)} - x_{(GT)}, \qquad (A.3)$$

424 where $E\left[\Delta F\left(X_{(GT)}(t)\right) | \vec{X}(t) = \vec{x}\right]$ is the conditional expected value for change in the function

425 F of the random variable given that $\vec{X}(t) = (X_R(t) \quad X_M(t) \quad X_{RR}(t) \quad X_{RM}(t) \quad X_{MM}(t))^T$

426 equals $\vec{x} = (x_R \quad x_M \quad x_{RR} \quad x_{RM} \quad x_{MM})^T$.

427   To simplify this fully stochastic system, we assume that the resident population is large

428 and treat demographic changes deterministically prior to the appearance of the mutation.

429 Considering the dynamics of the resident population, we then find the equilibrium of these

430 dynamical equations by solving $N_{tot} q_R - \hat{x}_R = 0$ and $N_{tot} q_{RR} - \hat{x}_{RR} = 0$ $(\hat{x}_R + \hat{x}_{RR} = N_{tot})$.

431 Setting $\hat{x}_R = \hat{\rho}_H^G N_{tot}$ and $\hat{x}_{RR} = \hat{\rho}_D^G N_{tot}$, the fraction of haploids $\hat{\rho}_H^G$ (and diploids $\hat{\rho}_D^G = 1 -$

432 $\hat{\rho}_H^G$) at equilibrium becomes,

$$\hat{\rho}_H^G = \frac{a_H w_R + a_D w_{RR} - 2w_{RR} + \sqrt{4(1-a_H)(1-a_D)\tilde{w}_R w_{RR} + (a_H w_R - a_D w_{RR})^2}}{2[a_H w_R + (1-a_H)\tilde{w}_R - w_{RR}]}, \qquad (A.4)$$

433 where $\tilde{w}_R = f_R w_R / 2$ is the fitness of haploids considering the cost of sex (see Supplementary

434 *Mathematica* file for the step-by-step derivation). We note that, when the fertility of haploids is

435 much greater than that of diploids ($w_R \gg w_{RR}$), the frequency of haploids in a population

436 approaches $a_H / \{a_H + [(1-a_H)f_R / 2]\}$, which is less than one because sexual reproduction of

437 the haploids produces diploids (the $(1-a_H)f_R / 2$ term). Conversely, when the fertility of

21

438   diploids is much greater than haploids ($w_R \ll w_{RR}$), the frequency of haploids approaches $1 -$

439   a_D, the rate at which diploids undergo meiosis.

440

441   A.2. First moment of change in allele frequency

442   To derive the first moment of change in allele frequency, $m^{Model}(p_{ave})$, we apply a

443   separation of time scales (e.g., Nagylaki 1976; Otto and Day 2007; Bessho and Otto 2017).

444   Details of the calculation are represented in the Supplementary *Mathematica* file. We first

445   transform the expected change in the number of individuals of each type (five variables that sum

446   to N_{tot}) into the expected change in a new set of four variables, $\Theta \in \{p_{ave}, \delta_p, \eta_{HW}, \rho_H\}$,

447   described by the functions:

$$\mathrm{E}\left[\Delta\Theta | \vec{X}(t) = \vec{x}\right] = f_\Theta^{Model}\left(\epsilon, p_{ave}, \vec{\theta}\right), \tag{A.5}$$

448   where $\vec{\theta} = \left(\delta_p, \eta_{HW}, \rho_H\right)$ and ϵ is proportional to the selection coefficients and assumed small

449   (the functions f are given explicitly in the Supplementary *Mathematica* file). With local

450   regulation, ρ_H is assumed fixed at N_H/N_{tot} and dropped from the variable set, Θ.

451   To constant order (setting the small changes due to selection to zero, $\epsilon \to 0$), the fast

452   ecological dynamics of the system are described by: $f_\Theta^{Model}\left(0, p_{ave}, \vec{\theta}\right)$. This system of

453   equations rapidly approaches a steady state found by solving $f_\Theta^{Model}\left(0, p_{ave}, \vec{\theta}\right) = 0$, which

454   gives $\bar{\delta}_p = \bar{\eta}_{HW} = 0$, and $\bar{\rho}_H = \hat{\rho}_H^G$ (Eq. A.4). To this order, the steady state change in allele

455   frequency is zero, $f_{p_{ave}}^{Model}\left(0, p_{ave}, \vec{\theta}\right) = 0$. We then describe slower changes, including changes

456   in allele frequency due to selection, by describing the deviations that occur around this steady

457   state. Specifically, to order ϵ, the variables are allowed to deviate from the steady state by $\delta_p =$

458    $\tilde{\delta}_p \epsilon$, $\eta_{HW} = \tilde{\eta}_{HW} \epsilon$, and $\rho_H = \hat{\rho}_H^G + \tilde{\rho}_H \epsilon$, and the dynamics $f_\Theta^{Model}\left(\epsilon, p_{ave}, \vec{\theta}\right)$ are then

459   approximated using a Taylor series expansion. Defining the average allele frequency by

460   combining haploid and diploid populations using an arbitrary weighting, $p_{ave} = \omega p_H +$

461    $(1 - \omega)p_D$, we show in the Supplementary *Mathematica* file that setting the weights proportional

462   to the class reproductive values (given by Eq. (2) with global regulation and Eq. (5) with local

463   regulation) is the only choice that separates evolutionary change in p_{ave} from changes in the

464   other variables to order ϵ. Defining the average allele frequency in this way (Eq. 1a) and taking

465   the Taylor series, the change in allele frequency becomes:

$$\mathrm{E}\big[\Delta p_{ave}|\vec{X}(t) = \vec{x}\big] \approx M^{Model}(p_{ave}) \tag{A.6}$$

$$= \frac{p_{ave}(1 - p_{ave})}{2}\Big[2s_{ave}^{Model} + 2c_D^{Model}p_{ave}(1 - 2h)s_{MM}^{w}\Big].$$

466

467   A.3. Second moment of change in average allele frequency

468   We next derive the second moment of change in average allele frequency in a haploid-

469   diploid population with asexuality. We again assume that the population size is very large, that

470   selection is very weak, and that the system has approached the steady state in $\big(\delta_p, \eta_{HW}, \rho_H\big)$,

471   ignoring deviations that are of $O(\epsilon)$. Because selection is assumed weak, the second moment is

472   well approximated by that of the neutral model (to constant order, $\epsilon \to 0$).

473   Under these assumptions, the fraction of haploids in a population is relatively fixed in

474   both the global and local regulation models, and we can sample the haploid offspring according

475   to a binomial distribution, with expectation and variance: $\mathrm{E}\big[X_M|\vec{X}(t) = \vec{x}\big] = q_M N_H$ and

476    $\mathrm{Var}\big[X_M|\vec{X}(t) = \vec{x}\big] = q_M(1 - q_M)N_H$ where $q_M = b_M/(b_R + b_M)$. To simplify the equation,

477   we set $\mathrm{E}\big[X_{(GT)}|\vec{X}(t) = \vec{x}\big] = m_{(GT)}$ and $\mathrm{Var}\big[X_{(GT)}|\vec{X}(t) = \vec{x}\big] = v_{(GT)}$, finding that:

$$\mathrm{E}\big[\Delta X_M|\vec{X}(t) = \vec{x}\big] = m_M - x_M, \tag{A.7a}$$

$$\mathrm{E}\big[(\Delta X_M)^2|\vec{X}(t) = \vec{x}\big] = v_M + m_M^2 - 2m_M x_M + x_M^2. \tag{A.7b}$$

478   In terms of allele frequencies (rather than numbers), we have the first and second moments for

479   the haploid offspring population, $E\left[\frac{\Delta X_M}{N_H}|\vec{X}(t) = \vec{x}\right] = \frac{1}{N_H}E\left[\Delta X_M|\vec{X}(t) = \vec{x}\right]$ and

480    $E\left[\left(\frac{\Delta X_M}{N_H}\right)^2|\vec{X}(t) = \vec{x}\right] = \frac{1}{N_H^2}E\left[(\Delta X_M)^2|\vec{X}(t) = \vec{x}\right].$

481   Similarly, the diploid offspring are sampled according to a trinomial distribution, with

482   expectation, variance, and covariance: $m_{(GT)} = q_{(GT)}N_D$, $v_{(GT)} = q_{(GT)}\left(1 - q_{(GT)}\right)N_D$, and

483    $Cov\left[X_{RM}, X_{MM}|\vec{X}(t) = \vec{x}\right] = q_{RM}q_{MM}N_D$, where $q_{(GT)} = b_{(GT)}/(b_{RR} + b_{RM} + b_{MM})$. To derive

484   the moments of the allele frequency in diploids, we define, $y_M = (x_{RM}/2) + x_{MM}$ and $Y_M =$

485    $(X_{RM}/2) + X_{MM}$. The moments of random variable Y are then:

$$E\left[Y_M|\vec{X}(t) = \vec{x}\right] = \frac{m_{RM}}{2} + m_{MM}, \tag{A.8a}$$

$$E\left[Y_M^2|\vec{X}(t) = \vec{x}\right] = \frac{v_{RM} + m_{RM}^2}{4} + \left(Cov\left[X_{RM}, X_{MM}|\vec{X}(t) = \vec{x}\right] + m_{RM}m_{MM}\right) + (v_{MM} + m_{MM}^2), \tag{A.8b}$$

$$E\left[\Delta Y_M|\vec{X}(t) = \vec{x}\right] = \frac{E\left[\Delta X_{RM}|\vec{X}(t) = \vec{x}\right]}{2} + E\left[\Delta X_{MM}|\vec{X}(t) = \vec{x}\right] - y_M, \tag{A.8c}$$

$$E\left[(\Delta Y_M)^2|\vec{X}(t) = \vec{x}\right] = E\left[Y_M^2|\vec{X}(t) = \vec{x}\right] - 2E\left[Y_M|\vec{X}(t) = \vec{x}\right]y_M + y_M^2. \tag{A.8d}$$

486   To consider the change in average allele frequency across the entire population, we

487   define $Z_M = c_H^{Model}\frac{X_M}{N_H} + c_D^{Model}\frac{Y_M}{N_D}$ and consider the expectation of change in this random

488   variable. Plugging in Eqs. (7a), (7b), (8c), and (8d), we have

$$E\left[(\Delta Z_M)^2|\vec{X}(t) = \vec{x}\right] = \frac{p_{ave}(1 - p_{ave})\left[\left(c_D^{Model}\right)^2\hat{\rho}_H^{Model} + \left(c_H^{Model}\right)^2\left(2\hat{\rho}_D^{Model}\right)\right]}{\hat{\rho}_H^{Model}\left(2\hat{\rho}_D^{Model}\right)N_{tot}}. \tag{A.9}$$

489   After transforming time scales using the variable $\tau = t/N_{tot}$ and defining $P(\tau) = Z(N_{tot}\tau)$,

490   we have the diffusion coefficient $v^{Model}(p_{ave}) = \lim_{N_{tot}\to\infty}E\left[\frac{(P(\tau+\Delta\tau)-P(\tau))^2}{\Delta\tau}\right]$ by taking the limit

491    $N_{tot} \to \infty$, giving Eq. (3c). Similarly, we derive the drift coefficient using Eq. (A6) ($m^{Model} =$

492    $M^{Model}N_{tot}$), giving Eq. (3b).

493

24

References

Bell, G. 1982. The Masterpiece of Nature: The Genetics and Evolution of Sexuality. University of California Press. Berkeley, CA.

Bell, G., 1994. The comparative biology of the alternation of generations. Lectures on mathematics in the life sciences 25, 1–26.

Bessho, K., Otto, S. P. 2017. Fixation probability in a haploid-diploid population. Genetics 205, 421-440.

Comai, L. 2005. The advantages and disadvantages of being polyploid. Nature Reviews Genetics 6, 836-846.

Coelho, S. M., Peters, A. F., Charrier, B., Roze, D., Destombe, C., Valero, M., Cock, J. M., 2007. Complex life cycles of multicellular eukaryotes: new approaches based on the use of model organisms. Gene 406, 152–170.

Crow, J. F., Kimura, M. (1970). An introduction to population genetics theory. The Blackburn Press, New Jersey.

Deithier, M. N. (1981). Heteromorphic algal life histories: The seasonal pattern and response to herbivory of the brown crust, *Ralfsia californica*. Oecologia 49, 333-339.

Destombe, C., Godin, J., Nocher, M., Richerd, S., Valero, M. (1993). Differences in response between haploid and diploid isomorphic phases of *Gracilaria verrucosa* (Rhodophyta: Gigartinales) exposed to artificial environmental conditions. Hydrobiologia 260/261, 131-137.

De Wreede, R. E., Klinger, T. 1988. Reproductive strategies in algae. Plant reproductive ecology: Patterns and strategies, 267-284.

Drew, K. M. (1949). Conchocelis-phase in the life-history of *Porphyra umbilicalis* (L.) Kütz. Nature 164, 748-749.

Dyck, L. J., De Wreede, R. E. (2006). Seasonal and spatial patterns of population density in the marine macroalga *Mazzaella splendens* (Gigartinales, Rhodophyta). Phycological Research, 54(1), 21-31.

Goldstein, D. B. 1992. Heterozygote advantage and the evolution of dominant diploid phase. Genetics 132, 1195–1198.

Haghes, J. S., Otto, S. P. 1999. Ecology and the evolution of biphasic life cycles. The American Naturalist 154, 306–330.

Hannach, G., Santelicesm, B. 1985. Ecological differences between the isomorphic reproductive phases of two species of *Iridaea* (Rhodophyta: Gigartinales). Marine Ecology Progress Series 22, 291–303.

Hawkes, M. W. 1990. Reproductive strategies. Biology of the red algae, 455-476.

529   Immler, S., G. Arnqvist, and S. P. Otto. 2012. Ploidally antagonistic selection maintains stable
530   genetic polymorphism. 66:55–65.
531   Jenkins, C. D., Kirkpatrick, M., 1995. Deleterious mutation and the evolution of genetic life
532   cycles. Evolution, 512–520.
533   Karlin, S. 1968. Rates of approach to homozygosity for finite stochastic models with variable
534   population size. The American Natualist 102, 443-455.
535   Kimura, M., 1957. Some problems of stochastic processes in genetics. The Annals of
536   Mathematical Statistics, 882-901.
537   Kimura, M., 1962. On the probability of fixation of mutant genes in a population. Genetics 47,
538   713.
539   Mable, K. B., Otto, P. S., 1998. The evolution of life cycles with haploid and diploid phases.
540   BioEssays 20, 453–462.
541   Nagylaki, T., 1976. The evolution of one-and two-locus systems. Genetics 83, 583-600.
542   Orr, H. A., Otto, S. P. 1994. Does diploidy increase the rate of adaptation? Genetics 136, 1475–
543   1480.
544   Otto, S., Goldstein, D., 1992. Recombination and the evolution of diploidy. Genetics 131, 745–
545   751.
546   Otto, S., 1994. The role of deleterious and beneficial mutations in the evolution of ploidy levels.
547   Lectures on Mathematica in the Life Sciences 25, 69–98.
548   Otto, S. P., Marks, J. C. 1996. Mating system and the evolutionary transition between haploidy
549   and diploidy. Biological Journal of the Linnean Society 57, 197-218.
550   Otto, S. P., Day, T., 2007. A biologist's guide to mathematical modeling in ecology and
551   evolution. Princeton University Press.
552   Otto, S. P., Whitton, J. 2000. Polyploid incidence and evolution. Annu. Rev. Genet. 34, 401-437.
553   Perrot, V., Richerd, S., Valéro, M., 1991. Transition from haploidy to diploidy. Nature 351, 315–
554   317.
555   Ramsey, J., Schemske, D. W. 1998. Pathways, mechanisms, and rates of polyploid formation in
556   flowering plants. Annual reviews of Ecology and Systematics 29: 467-501.
557   Raper, J. R., Flexer, A. S. (1970). The road to diploidy with emphasis on a detour. In *Symp. Soc.*
558   *Gen. Microbiol* (Vol. 20, pp. 401-432).
559   Rousset, F. (2004). Genetic structure and selection in subdivided populations. Princeton
560   University Press, New Jersey.
561   Scott, M. F., Rescan, M. 2016. Evolution of haploid-diploid life cycles when haploid and diploid
562   fitnesses are not equal. Evolution 71, 215–226.
563   Slatkin, M. 1987. Gene flow and the geographic struture of natural populations. Science New
564   Series 236: 787-792.

565   Slocum C. J. 1980. Differential susceptibility to grazers in two phases of an intertidal alga:
566   Advantages of heteromorphic generations. Journal of Experimental Marine Biology and
567   Ecology 46, 99-110.

568   Taylor, P. D. 1980. Allele-Frequency Change in a Class-Structured Population. The American
569   Naturalist 135, 95-106.

570   Thornber, C. S., Gains, S. D. 2004. Population demographics in species with biphasic life cycle.
571   Ecology 85, 1661-1674.

572   Thornber, C., Stachowicz, J. J., Gains, S. 2006. Tissue type matters: selective herbivory on
573   different life history stages of an isomorphic alga. Ecology 87, 2255-2263.

574   Vieira, V. M. N. C. S., Engelen, A. H., Huanel, O. R., Guillemin, M. 2018a. Haploid females in
575   the isomorphic biphasic life-cycle of *Graciaria chilensis* excel in survival. BMC
576   Evolutionary Biology 18:174.

577   Vieira, V. M. N. C. S., Engelen, A. H., Huanel, O. R., Guillemin, M. 2018b. Differentiation of
578   haploid and diploid fertilities in *Gracilaria chilensis* affect ploidy ratio. BMC
579   Evolutionary Biology 18:183.

580   Willson, M. F. 1981. On the evolution of complex life cycles in plants: a review and an
581   ecological perspective. Annals of the Missouri Botanical Garden 68, 275-300.

582

583   **Figure Captions**

584   Fig. 1. An illustration of the haploid-diploid models. (a) In the global regulation model, both

585   haploids and diploids occupy the same habitat and density dependence holds the total population

586   size N_{tot} constant. (b) In the local regulation model, each ploidy stage occupies a different

587   habit, therefore density dependence regulates the population size of haploids (N_H) and diploids

588   (N_D) separately.

589

590   Fig. 2. Class reproductive value of haploids in the global regulation model, c_H^G. Curves show c_H^G

591   as a function of the degree of haploid asexuality, a_H (x-axis), with the degree of diploid

592   asexuality ranging in color from $a_D = 0.05$ (red) to 0.95 (blue) in increments of 0.05. Other

593   parameters are set as: (a) $f_R = 0.5$, $w_R = 5000$, $w_{RR} = 1000$, (b) $f_R = 0.5$, $w_R = 1000$,

594   $w_{RR} = 5000$. The resulting frequency of haploids, $\hat{\rho}_H^G$ (Eq. A.4), is shown in the inset plots.

27

595

596   Fig. 3. Proportional reproductive value of haploids in the local regulation model, c_H^L. Parameters

597   are the same as Fig. 2, except that haploids are held fixed at a frequency of (a)(b) $\hat{\rho}_H^L = 0.8$ or

598   (c)(d) $\hat{\rho}_H^L = 0.3$. We consider the case when (a)(c) haploid fitness parameter is larger than

599   diploid $w_R = 5000$, $w_{RR} = 1000$ ($w_H > w_D$), and when (b)(d) diploid fitness parameter is

600   larger than haploid $w_R = 1000$, $w_{RR} = 5000$ ($w_H < w_D$).

601

602   Fig. 4. The effective population size of a haploid-diploid population. The relative effective

603   population size over the total population size (N_e^{Model}/N_{tot}, Eq. 7) is shown as a function of the

604   frequency of haploids ($\hat{\rho}_H^{Model}$, x-axis), when the haploid reproductive value (c_H^{Model}) varies from

605   0.05 (blue) to 0.95 (red) in increments of 0.05. This figure applies to both global and local

606   regulation models.

607

608   Fig. 5.   The effective population size of a haploid-diploid population in the global regulation

609   model as a function of the degree of asexuality, a_H and a_D. Parameters are the same as in Fig. 2

610   and determine the relative class reproductive values (c_H^G) and fraction of haploids ($\hat{\rho}_H^G$) according

611   to Eqs. (2a) and (A.4).

612

613   Fig. 6. The effective population size of a haploid-diploid population in the local regulation

614   model. Parameters are the same as in Fig. 3 and determine the relative class reproductive values

615   (c_H^L) by Eqs. (5). The frequencies of haploids are held fixed at a frequency of (a)(b) $\hat{\rho}_H^L = 0.9$,

616   (c)(d) $\hat{\rho}_H^L = 0.8$, (e)(f) $\hat{\rho}_H^L = 0.6$, or (g)(h) $\hat{\rho}_H^L = 0.3$.

617

618   Fig. 7. Fixation probability given the average strength of selection, s_{ave}^{Model}, for global (a) and

619   local (b) regulation models. The solid curve gives the analytical result from the diffusion

620   approximation (Eq. (11)) and the dashed curve gives the linear approximation (Eq. (9b)). Black

621   dots indicate the fixation probability estimated from 10000 numerical simulations with 95% CI

622   (Wilson score interval for binomial). Parameters: $N_{tot} = 90$, $N_H = 60$, $N_D = 30$, $f_R = 0.5$,

623    $w_R = w_{RR} = 1000$, $a_H = a_D = 0.1$, $h = 0.5$, $s_M^f = 0$, $s_M^w = s_{RM}^w = s_{ave}^{Model}$, such that the

624   fraction of haploids in the resident population is $\hat{\rho}_H^{Model} = 2/3$ and class reproductive values

625   are equal $c_H^{Model} = c_D^{Model} = 1/2$. Holding $s_{ave}^{Model} = 1/2(s_M^w + s_{RM}^w)$ constant, similar results

626   are obtained for a range of different choices of s_M^w and s_{RM}^w (see supplementary *Mathematica*

627   file).

628

629   Fig. 8. The fixation probability in a haploid-diploid population in the global regulation model.

630   Curves gives the linear approximation for the fixation probability (Eq. (9a)). Parameters are the

631   same as in Fig. 2. Selection acts only in the haploid or diploid phase, with selection coefficients

632   set as $s_M^w = 0.02$ for haploid selection (a)(b) and $s_{RM}^w = 0.02$ for diploid selection (c)(d).

633

634   Fig. 9. The fixation probability in a haploid-diploid population in the local regulation model.

635   Curves gives the linear approximation for the fixation probability (Eq. (9a)). Parameters are the

636   same as in Fig. 3 and Fig. 8. The frequency of haploids is held fixed at (a)(b)(e)(f) $\hat{\rho}_H^L = 0.8$,

637   (c)(d)(g)(h) $\hat{\rho}_H^L = 0.3$. Fitness of haploids is higher than diploids in panels (a)(c)(e)(g) ($w_H >$

638   w_D), and the opposite condition is considered in panels (b)(d)(f)(h) ($w_H < w_D$). Selection only

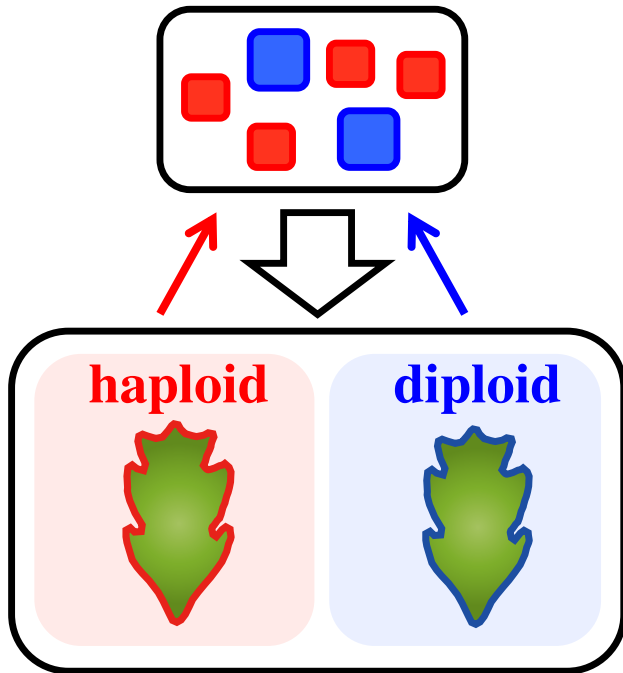639   occurs in the haploid (a)(b)(c)(d) or diploid stage (e)(f)(g)(h).

640

641   **Supporting information**

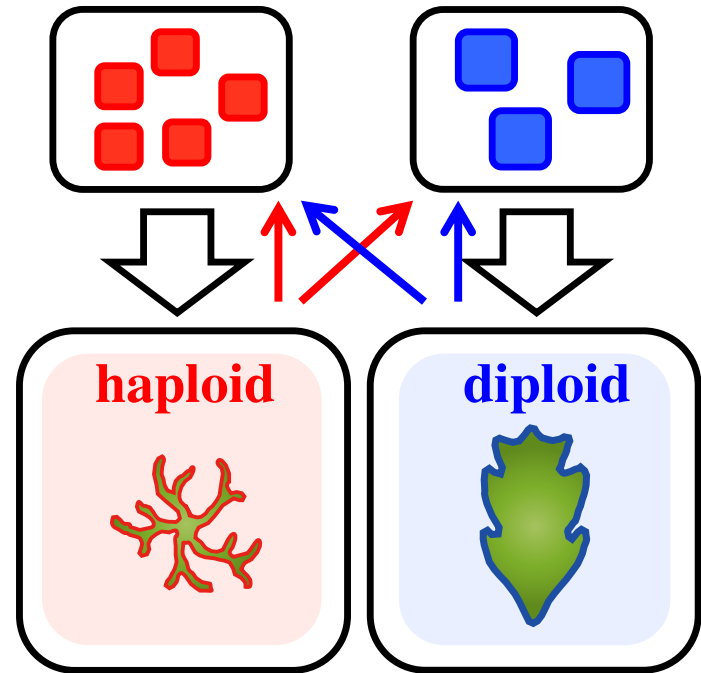642   S1. Supplementary *Mathematica* file.

Figure1

(a)

Global regulation

haploid   **diploid**

Total population size: N_{tot}

(b)

Local regulation

haploid   **diploid**

N_{H} N_{D}

Bessho and Otto

Figure 2

Bessho and Otto

Figure 3

Bessho and Otto

Figure 4

$$\frac{N_e^{Model}}{N_{tot}}$$

small $\hat{c}_H^{Model}$

large $\hat{c}_H^{Model}$

$\hat{\rho}_H^{Model}$

Bessho and Otto

Figure 5

$$\frac{N_e^{Model}}{N_{tot}}$$

(a) $\quad w_H > w_D$

small a_D

large a_D

a_H

(b) $\quad w_H < w_D$

a_H

Bessho and Otto

Figure 6

(a) $w_H > w_D$

(b) $w_H < w_D$

small a_D

large a_D

$\hat{\rho}_H^L = 0.9$ $\dfrac{N_e^{Model}}{N_{tot}}$

(c)

(d)

$\hat{\rho}_H^L = 0.8$ $\dfrac{N_e^{Model}}{N_{tot}}$

(e)

(f)

$\hat{\rho}_H^L = 0.6$ $\dfrac{N_e^{Model}}{N_{tot}}$

(g)

(h)

$\hat{\rho}_H^L = 0.3$ $\dfrac{N_e^{Model}}{N_{tot}}$
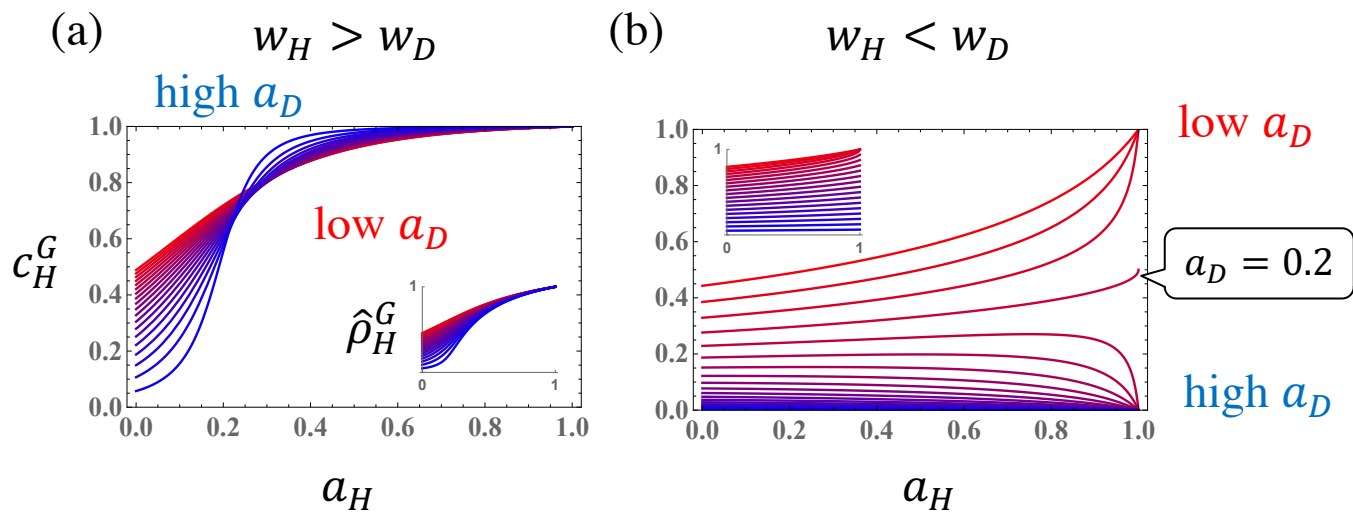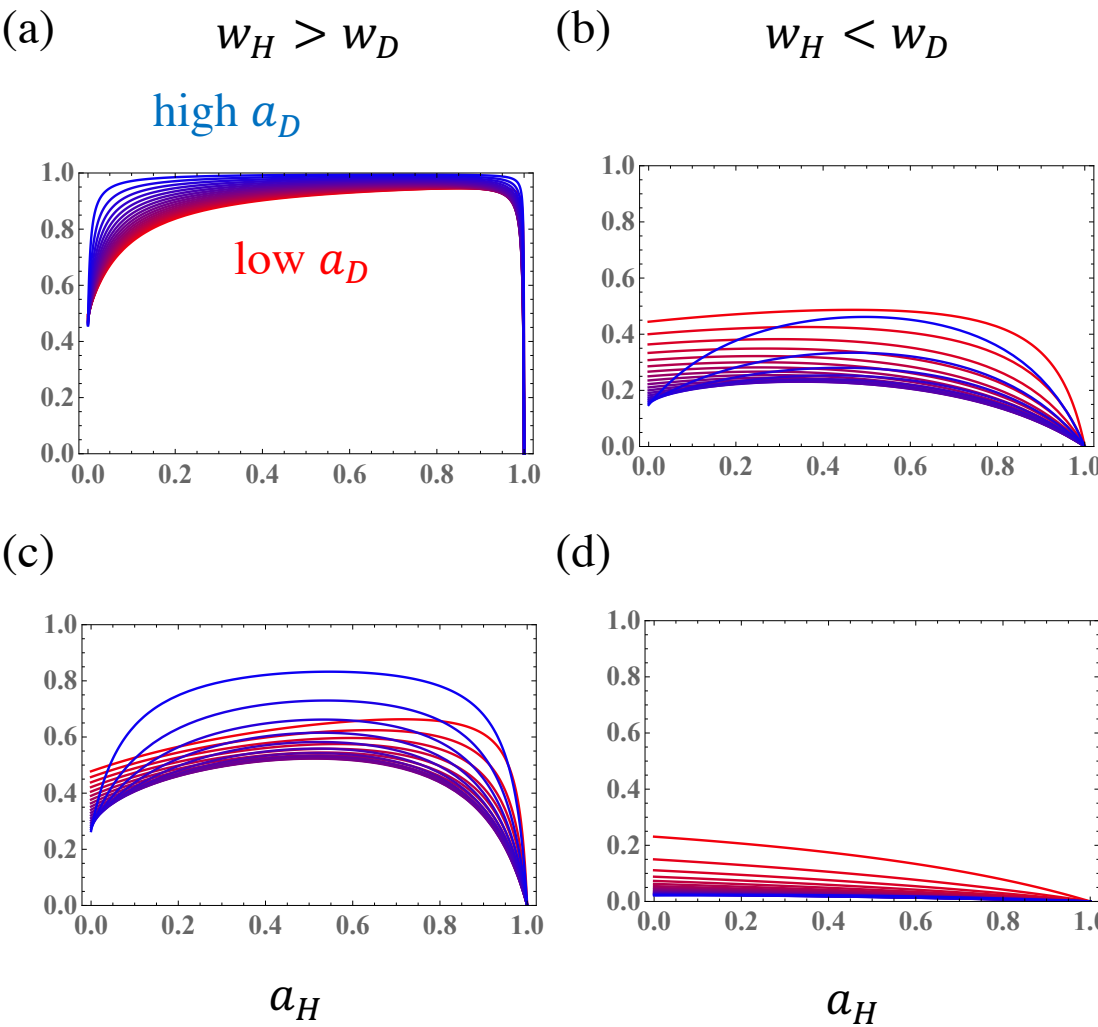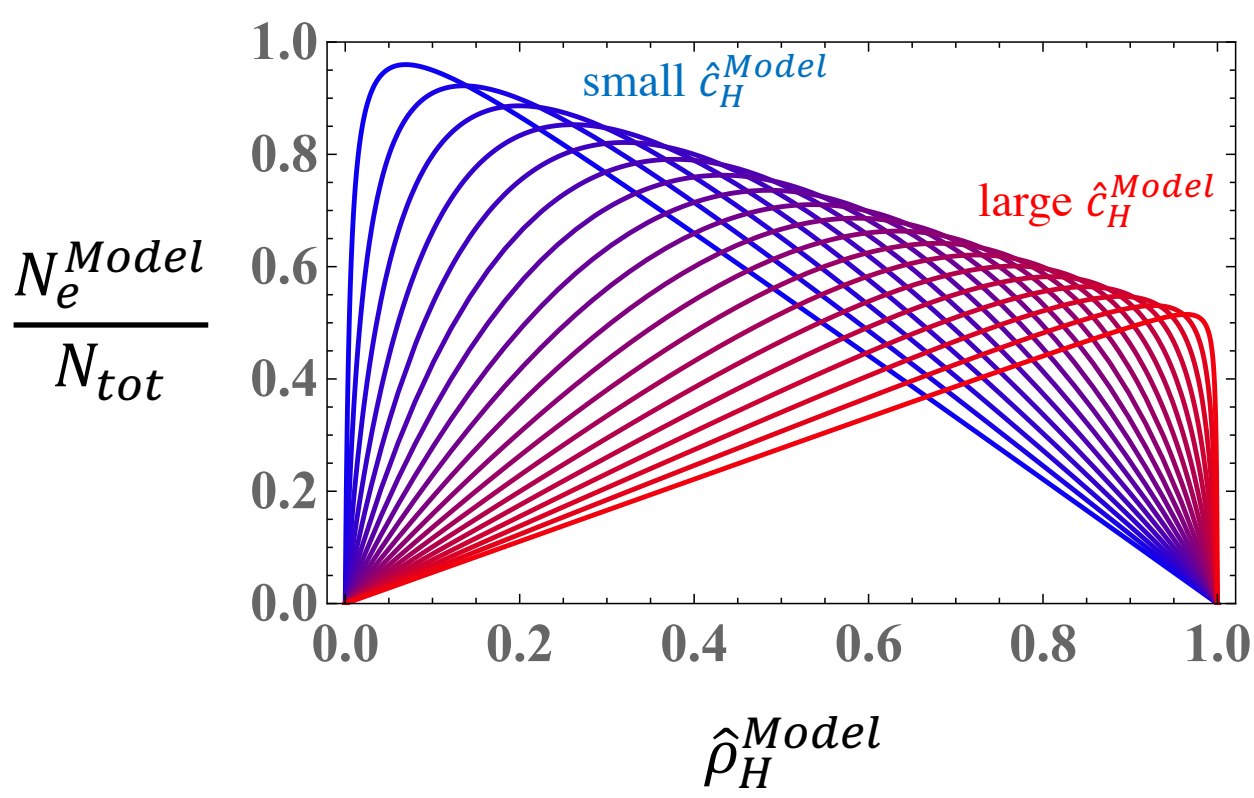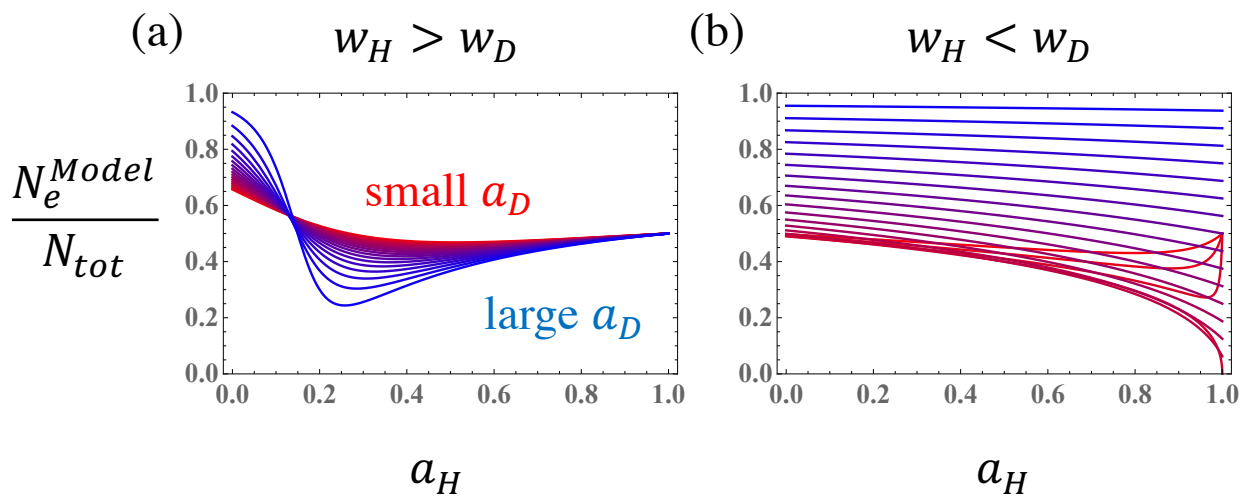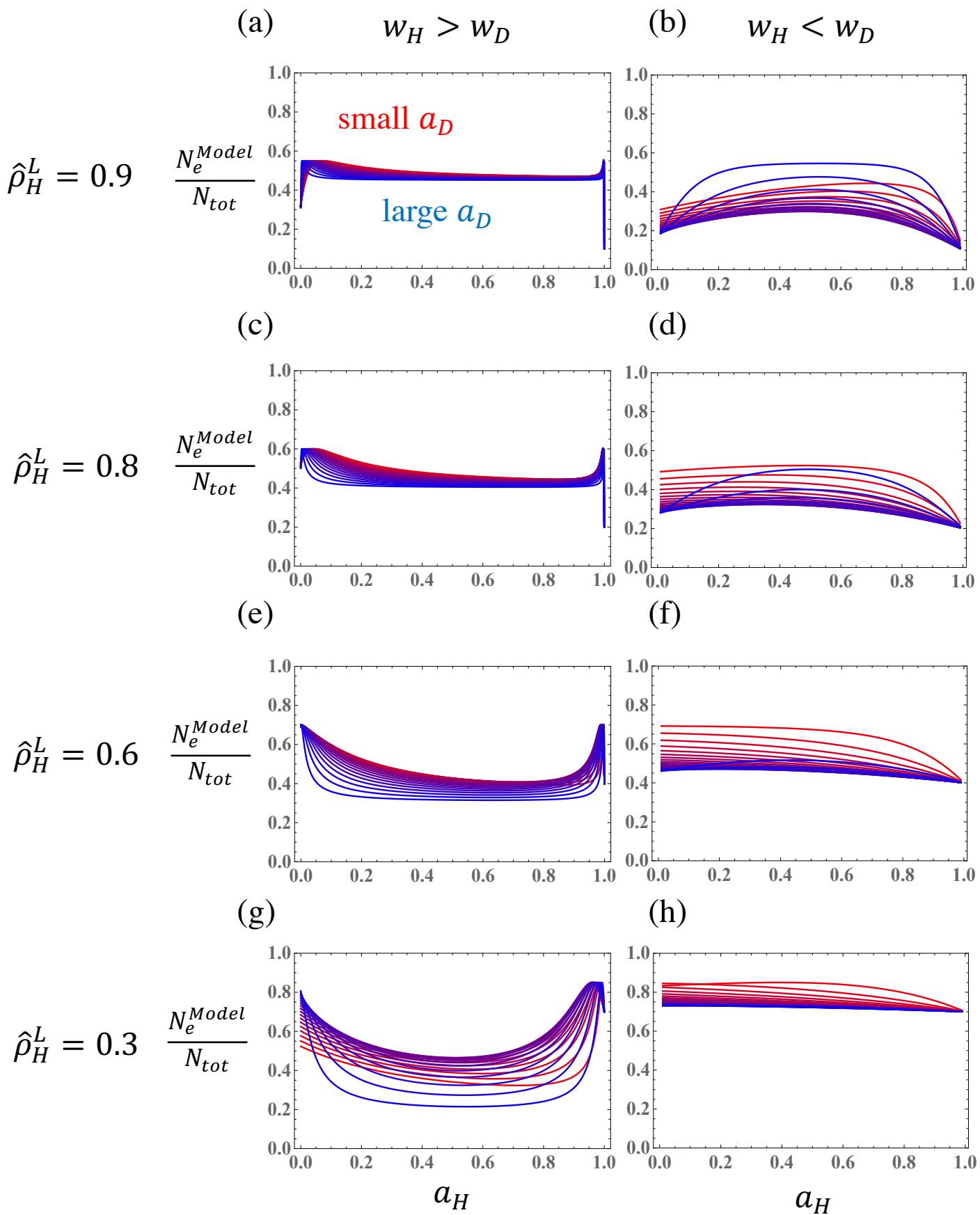
a_H a_H

Figure 7

(a) global regulation

(b) local regulation

Bessho and Otto

Figure 8

Bessho and Otto

Figure 9

(a) $w_H > w_D$

(b) $w_H < w_D$

$\hat{\rho}_H^L = 0.8 \quad u$

low a_D

high a_D

Haploid selection

(c)

(d)

$\hat{\rho}_H^L = 0.3 \quad u$

(e) $w_H > w_D$

(f) $w_H < w_D$

$\hat{\rho}_H^L = 0.8 \quad u$

Diploid selection

(g)

(h)

$\hat{\rho}_H^L = 0.3 \quad u$

a_H

a_H